JOURNAL OF MATERIALS SCIENCE 11 (1976) 1439–1449

Application of high resolution autoradiography to study the microsegregation of carbon in thin foil microstructures of a 12% Cr steel using ^{14}C as a radioactive tracer

G. V. PRABHU GAUNKAR, A. M. HUNTZ, P. LACOMBE
Laboratoire de Métallurgie, Université Paris-Sud, Centre d'Orsay, 91405 Orsay, France

The technique of high resolution microautoradiography has already been applied to study the microsegregation of carbon and tritium in iron and its alloys, but autoradiographs have so far been obtained using liquid nuclear emulsions and carbon replicas on massive specimens. This technique has now been extended to study the distribution of carbon in thin foil microstructures of a 12% chromium steel in the quenched and tempered condition. An experimental procedure has been developed for obtaining autoradiographs on thin foils, and is described in detail. The limitations of the technique with respect to efficiency and resolution have been considered. The results obtained show that high resolution microautoradiography on thin foils permits a more precise localization of the radioactive tracer atoms with respect to the microstructural features and gives a better resolution, even with a radioisotope emitting high energy β particles, in comparison with the replica method on massive specimens.

1. Introduction

The autoradiographic methods using liquid nuclear emulsions have been adopted to study the microsegregation of radioactive tracer atoms in complex metallic microstructures because of the excellent resolution that liquid nuclear emulsions can give [1–3]. It was found that the limit of resolution in the case of autoradiographs, obtained on the replicas from massive specimens, was of the order of 3000 Å for strongly ionizing radiations (β particles from H^3; $E_{max} = 18$ keV) [1] and of the order of 4 to 10 μm for more energetic radiations (β particles from ^{14}C; $E_{max} = 155$ keV) [1–3]. The difference in the limitations of resolution is related to the mean course of the radiations; when a radioactive tracer emits β-particles of higher energy, sources situated deeper in a specimen will also be effective in activating silver bromide crystals situated over large horizontal distances from the source, thus leading to a poorer resolution (cf. Fig. 5). Hence if one wants to improve the limit of resolution of the autoradiographs, especially when radioactive tracers emitting high energy radiations (^{14}C, ^{35}S, ^{32}P) are used, the distance between the emulsion and the sources should be reduced to low values. This can be done by using thin foils instead of massive specimens. The use of thin foils gives an additional advantage in that the microstructure can be observed directly by transmission electron microscopy with an autoradiograph superimposed.

Considering the importance of the role of carbon in phase transformations and the autoradiographic techniques using ^{14}C employed so far [1–6], an attempt has been made to develop a technique for obtaining autoradiographs on thin foils of a steel charged with ^{14}C [7, 8]. A 12% chromium steel has been chosen as a material for investigations in the present work with a view to studying the role of carbon during tempering of martensite.

In this paper the experimental technique developed for obtaining high resolution microautoradiographs on thin foils is described in detail,

the limitations of the technique with respect to efficiency and resolution are considered and its application in studying the role of carbon during tempering of martensite of a 12% Cr steel is discussed.

2. Experimental procedure

2.1. Materials

Chemical analysis of the 12% Cr steel* used in the present work is given in Table I. Rectangular specimens of dimensions 15 mm x 50 mm were cut from sheets rolled down to a thickness of 0.1 mm.

TABLE I Chemical composition of the steel

	C	Si	Mn	Cr
(wt%)	0.10	1.0	1.0	12.7

2.2. Charging the specimens with ^{14}C and heat-treatments

To charge with ^{14}C, a specimen was sealed in an evacuated silica capsule together with about 1 mg of barium carbonate, marked with radioactive carbon (specific activity $\approx 0.25\ mCi\ mg^{-1}$) contained in a tiny glass capillary tube, and was heated at 1200° C for 45 min. Cementation of the specimen with radioactive carbon takes place, possibly with the help of the following reactions: [2]

$$BaCO_3 + SiO_2 \longrightarrow BaSiO_4 + CO\uparrow$$

$$2CO \longrightarrow CO_2\uparrow + C\ (metal).$$

About 10 ppm of radioactive carbon [2] are thus introduced into a specimen; this is a negligible quantity compared with the actual carbon content of the steel.

Specimens charged with ^{14}C were then heated at 1000° C for 40 h to bring about homogeneous distribution of the radioactive carbon. It was verified by densitometry on film autoradiographs (Lumilith) that this treatment gives homogeneous distribution of the radioactive carbon. The specimens were then austenitized in silica capsules, sealed under argon atmosphere, at 1025° C for 2 h. The specimens were quenched in water at the end of an austenitization, to obtain a martensitic structure as shown in Fig. 1. Some specimens were then tempered at different temperatures and water-quenched at the end of tempering.

* AFNOR $Z_{12}C_{13}$ grade from a commercial melt.

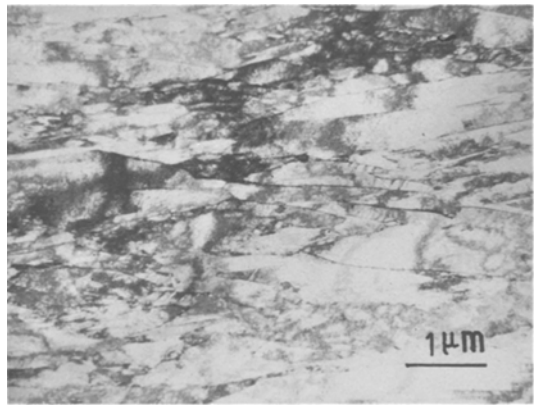

Figure 1 Thin foil microstructures of an as-quenched specimen of the 0.1% C–12% Cr steel (austenitized at 1025° C for 2 h and water-quenched) showing a typical lath martensite structure.

2.3. Preparation of thin foils

The heat-treated specimens were mechanically polished under water to remove any oxide layer that might have formed on the specimen surface during heat-treatment. Thin foils were then prepared by electrolytic thinning of the specimens in an acetochromic bath (acetic acid: 432 ml; chromic anhydride: 100 g; water: 25 ml; 13° C; 18 V). At the end of the thinning, the thin foils were collected, washed with distilled water and ethyl alcohol, and stored in the latter.

2.4. Autoradiography

The success of the experiments with high resolution electron microautoradiography [1, 2, 9], using a liquid nuclear emulsion, depends very much on the realization of a truly monogranular, densely packed layer of the emulsion, and the protection of the thin foils from any damage during handling or chemical attack. In order to render the manipulations simple and to reduce the possibilities of artefacts or damage, the following procedure was adopted.

(a) Preparations for depositing the emulsion: the thin foils were first dipped in a 2.5% solution of collodion in amyl acetate and placed carefully on glass slides previously covered on one side with a thin membrane of collodion. The glass slides were held in a vertical position for some time in order to allow excess collodion to run off. The amyl acetate quickly evaporates and the thin foils, covered with a layer of collodion, adhere to the slide surface.

Collodion plays a double role; it forms a protective layer around the thin foils, thereby protecting the latter from any chemical attack and also, as will be seen later, it helps in separating the thin foils along with the superimposed autoradiographs from the glass slides. The use of glass slides helps in easy handling of the thin foils, and also in obtaining a uniform layer of emulsion (cf. Fig. 3), since a film of emulsion can be deposited over a large surface of the glass slide.

(b) Depositing the emulsion: in the present experiments, Ilford L_4 nuclear emulsion was used.

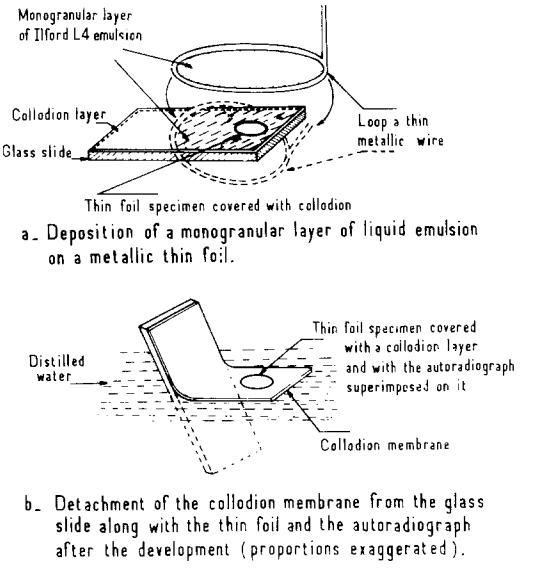

Figure 2 Schematic diagram illustrating some steps of the experimental procedure for obtaining autoradiographs on thin foils.

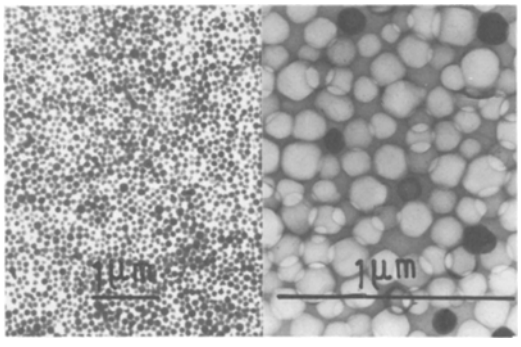

Figure 3 Emulsion layer as seen on an electron microscope; the AgBr crystals of the emulsion are reduced to silver grains by the electron beam and are seen as monogranular densely packed layer of silver grains (left half of the figure). During observations under the effect of the incident electron beam, the silver grains evaporate, leaving behind their traces in the gelatine (right half of the figure); note the slight overlapping of the images.

This emulsion gives a densely packed monogranular layer of silver bromide crystals when diluted to a concentration of 2 ml water per g emulsion [1] (Fig. 3). The emulsion was first melted at about 45° C, taking care to avoid any overheating, and was then diluted with the required amount of water. After dilution, it was held between 45 and 50° C for about 20 min to allow homogenization and was then cooled to room temperature (20° C). Very thin films of this emulsion may be obtained with the help of a loop of a thin metal wire. The film, thus obtained, is deposited on the surface of a glass slide containing thin foils (Fig. 2a). The emulsion is rapidly converted to gel form, thereby preventing any redistribution of the silver bromide crystals. The thin foils thus covered with a monogranular layer of the liquid nuclear emulsion (Fig. 3) were transferred to metallic containers and stored for an adequate time under an atmosphere of dry argon at −20° C. All manipulations with the nuclear emulsion were carried out in an inactinic orange light (Ilford S902 screen).

(c) Development of the autoradiographs: the containers in which the specimens are stored at −20° C were allowed to heat up to room temperature and the glass slides were taken out. The slides were then treated with a developer and a fixer successively. In the present work either D19 or para-phenylenediamine [1] were used as developers (time: 3 to 4 min). Development with D19 gives autoradiographs consisting of filaments (Fig. 4, average dimensions: 1600 Å), whereas treatment with para-phenylenediamine gives autoradiographs consisting of silver spheres (Fig. 4,

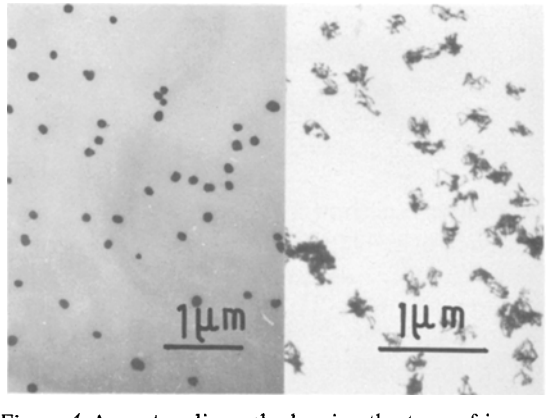

Figure 4 An autoradiograph showing the type of images obtained after the development of an autoradiograph with para-phenylenediamine (spheres: left half of the figure) and with D19 (filaments: right half of the figure).

average diameter: 900 Å) around the latent images. The spheres resulting from the latter developer, being smaller in dimensions, lead to a slightly better resolution and cover a smaller area of a thin foil microstructure; hence more structural detail can be observed. However, the duration of exposure to the β radiation, for obtaining an adequate number of silver grains on an autoradiograph using para-phenylenediamine, is longer than that for D19: in the present experiments, for specimens tempered at 700° C for 40 h, with an actual activity of 1.23×10^{-3} mCi cm^{-2}, the duration of exposure was 10 days for the autoradiographs developed with D19 (Fig. 14) and 70 days for the autoradiographs with para-phenylenediamine (Fig. 16a). The filaments resulting from D19 have an advantage over the spheres resulting from para-phenylenediamine because the former can always be identified with certainty whereas the spheres resulting from para-phenylenediamine may be confused with artefacts [1].

After treatment with a developer, the slides were rinsed with water, treated with a fixer for about 7 min and then rinsed again with water.

(d) Detachment of the thin foils: to detach thin foils from a glass slide, squares of appropriate dimensions were cut around the thin foils on the collodion membrane with a sharp scalpel. The slides were then slowly dipped, at an angle of about 45°, in distilled water. The squares of collodion membrane floated to the surface of the water (Fig. 2b) along with the thin foils and the autoradiographs. These were collected on a small piece of paper which contained a copper grid, such that the thin foil was placed exactly in the centre of the grid. The piece of paper was supported by a glass slide. The collodion membrane was then carefully cut around the grid and the grid was separated from the paper. The thin foil was then ready for observation along with its autoradiograph superimposed on it.

3. Analysis of the technique

The limit of resolution and the efficiency are the parameters that need to be considered for correct interpretation of the autoradiographs.

3.1. Efficiency

The efficiency of an autoradiograph may be defined as the ratio of the number of silver grains per unit area of an autoradiograph to the total number of β particles that enter the corresponding area of the emulsion during the time of exposure. If this factor is precisely determined, it will be possible to estimate the concentration of the radioactive atoms in a site of segregation.

The efficiency depends considerably on the nature of the energy spectrum of a radioactive isotope. The lower the energy of the β particles, the higher is their rate of loss of energy in a crystal of silver bromide along their track and hence the higher is the probability of their causing a latent image, which thus gives higher efficiency [9].

Efficiency also depends on the sensitivity of the emulsion [9]; Ilford L4 emulsion is found to give satisfactory results with ^{14}C as a radioactive tracer.

Another important factor affecting the efficiency, is the absorption of the β particles by the metal itself. The absorption of the β particles can be expressed by a relation of the type [2]

$$N_x = N_0(\tfrac{1}{2})x/d \qquad (1)$$

where N_x is the number of particles emerging from a surface situated at a distance x from a source. N_0 is the total number of particles emitted by a source, and d is a "semi-absorption" distance. It is observed that the value of N_x/N_0 is greater than 95% for a value of x/d less than ~ 0.1. In the present case, assuming the average value of x to be in the order of 2000 Å (cf. Fig. 5) and the value of d to be $\sim 3\,\mu$m (value for iron [1]), the value of x/d will be approximately equal to 0.07. The error involved if the effect due to absorption of the β particles in a thin foil is neglected will thus be less than 5%. It may be assumed that all the β particles emitted by the thin foil in the direction of the emulsion layer will reach the latter without any significant change in their energy value and hence the variations in the value of the efficiency due to the effect of the absorption of the β rays in a thin foil may be neglected.

The number of silver grains in an autoradiograph will be directly proportional to the number of the β particles entering the emulsion, which in turn depends on the thickness of the thin foil, the time of exposure of the autoradiographs and the activity of the specimen.

If n is the total number of disintegrations per second per unit volume (cm^3) of the thin foil material, causing the emission of n β particles in all possible directions, it can be assumed that $(n/2)$ β particles will enter the emulsion, since the area of the thin foil is large compared to its thickness. If r is the efficiency of an autoradiograph for

the emulsion used and the photographic process adopted, and t the total time of exposure in seconds, the number of silver grains per cm^2 of an autoradiograph will be equal to N (Ag), where

$$N(\mathrm{Ag}) = r\frac{n}{2}xt. \qquad (2)$$

Knowing the values of N (Ag), r, x and t it is possible to estimate the number of disintegrations and hence the number of radioactive atoms associated with a site of segregation such as a grain boundary. Knowledge of the values of efficiency and the activity of a specimen can be useful in determining the time of exposure required to obtain an optimum number of silver grains that will reveal the important sites of segregation but will not obliterate too many structural features.

It may be noted that not every β particle entering the emulsion gives rise to a silver grain. Furthermore, the possibility of the disintegration of a radioactive atom during a certain period of time is itself governed by a statistical probability. Hence, not all sites containing radioactive atoms will be revealed on an autoradiograph after a certain time of exposure.

3.2. The resolution of the autoradiographs

In the case of electron microscope autoradiography, the definition adopted equates the resolution to the radius of a circle traced on the surface of the emulsion, around a point source, which contains half the silver grains produced by the source [1, 2, 9].

In the case of electron microscope autoradiographs on thin foils, it is difficult to define the autoradiographs resolution on the basis of the grain density because the grains are very much individualized. It is also not desirable to have a large number of silver grains, even if it were possible to obtain it after a long time of exposure, because they would obliterate the essential microstructural features. This makes a definition of the limit of resolution more difficult. However, an analysis of the situation would give an approximate idea of the uncertainty that will be involved whilst associating the silver grains in an autoradiograph with the structural features.

The uncertainty results from two factors. The first factor is the fact that a β particle from a point source can hit one or more silver bromide crystals which may not lie immediately over the source, and hence will give rise to silver grains situated at an appreciable horizontal distance from a structural feature containing the radioactive source. This factor will be considered as a limit of geometric resolution, ρ_g. The second factor is the fact that a latent image produced by the passage of a β particle through a silver bromide crystal may not lie along the path of a β particle, and further, the silver grain developing from a latent image may not coincide with the silver bromide crystal. This factor will be considered as a limit of photographic resolution ρ_p.

3.2.1. The limit of geometric resolution

If we consider a point source, situated at a distance x from the emulsion layer, emitting N_0 particles per second in the whole space, the density of the silver grains, per unit surface of the emulsion, due to this source can be written as

$$\frac{dN}{dS} = \frac{N_0}{4\pi x^2} \cdot \cos^3\theta \qquad (3)$$

where θ is the angle between the vector joining source and the emulsion point considered, and the normal to the emulsion. According to this type of distribution around a source, 50% of the silver grains would lie within a cone that divides the upper space into two equal halves. The semi-apex angle of this cone would be equal to $\pi/3$.

If the probability of finding a silver grain due to a radioactive source is assumed to follow a distribution as shown in Fig. 5, the limit of geometric resolution may be defined as a horizontal distance from a point source corresponding to which there is a 50% probability of finding a silver grain. Considering that x is a statistical value of the distance which separates a source and the silver bromide

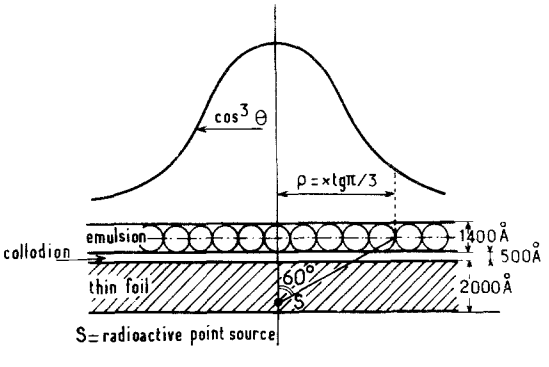

Figure 5 A curve showing the number of silver grains on an autoradiograph as a function of the horizontal distance ρ and illustrating the concept of the limit of geometric resolution for a point source.

crystal, the limit of geometric resolution will be equal to:

$$\rho_g = x \tan \frac{\pi}{3} = 1.7x, \qquad (4)$$

for a point source, where x is equal to the average distance between the AgBr crystal and the source (cf. Fig. 5),

$$x = \frac{1400}{2} + 500 + \frac{2000}{2} \simeq 2200 \text{ Å},$$

so

$$\rho_g = 3500 \text{ Å for a point source.}$$

If we consider a continuous source, such as an interface perpendicular to the surface of a thin foil, the number of silver grains within a distance ρ from an interface will be given by a relation:

$$dN = N \cdot \frac{\theta}{\pi} \cdot dx \qquad (5)$$

from which the number of Ag grains, $N(\rho)$, within a distance ρ from an interface can be expressed by the relation:

$$N(\rho) = \frac{N}{\pi}\left[\int_0^p \arctan\frac{\rho}{x}\,dx\right]$$

$$N(\rho) = \frac{N}{\pi}\left[p \operatorname{arc\,cot}\frac{p}{\rho} + \frac{\rho}{2}\log(\rho^2 + p^2) - \rho\log\rho\right] \qquad (6)$$

where p = thickness of a thin foil ($\simeq$ 2000 Å) and N = total number of silver grains due to the source.

For a value of ρ equal to infinity, $N(\rho)$ would be equal to $N(\rho_\infty) = Np/2$. Hence the number of silver grains corresponding to the limit of geometric resolution would be equal to $N(\rho_\infty)/2 = Np/4$. The value of ρ corresponding to this, i.e. ρ_g, can be shown from Equation 6, to be equal to $0.4p$; thus for thin foils, ρ_g will be of the order of 800 Å for a continuous source.

3.2.2. Limit of resolution due to the photographic process, ρ_p

As seen earlier, a latent image formed in a silver bromide crystal due to the passage of a β-particle may not necessarily lie along the path of the particle. A latent image can lie anywhere within an activated silver bromide crystal. Also, a silver grain developing from a latent image may grow in any direction and may not coincide with the parent silver bromide crystal. The situation is illustrated in Fig. 6 for development with D19, which gives silver filaments.

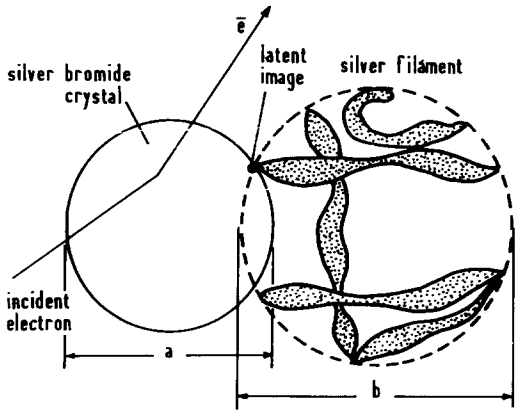

Figure 6 Figure illustrating the concept of the limit of photographic resolution [1].

The limit of resolution due to the photographic process may be expressed by the relation:

$$\rho_p = \sqrt{\left(\frac{a^2}{4} + \frac{b^2}{16}\right)} \qquad (7)$$

where a = diameter of the silver bromide crystals $\simeq$ 1400 Å for Ilford L4 emulsion, b = size of the developed grains $\simeq$ 1600 Å for the filaments of silver obtained with D19 and 900 Å for the spheres of silver obtained with para-phenylenediamine.

The values of ρ_p corresponding to the values of a and b mentioned above would be 850 and 750 Å for D19 and para-phenylenediamine respectively.

3.2.3. Overall limit of resolution

The total uncertainty due to the two limits of resolution will be equal to R, where

$$R = \sqrt{(\rho_g^2 + \rho_p^2)}. \qquad (8)$$

For a thin foil autoradiograph, the values of R would be of the order of 3700 Å with D19 as a developer for the point source, 3600 Å with para-phenylenediamine as a developer for a point source, 1300 Å with D19 as a developer for a continuous source, 1100 Å with para-phenylenediamine as a developer for a continuous source.

The values of the limit of resolution, measured on the autoradiographs shown in Figs. 14 and 16a are of the order of 1600 and 1100 Å for a continuous source (interfaces) with D19 and para-phenylenediamine as the respective developers and compare well with the predicted values.

The concept of the limit of resolution is useful

in knowing the certainty with which a silver grain on an autoradiograph can be associated with a structural feature assumed to contain a radioactive source corresponding to the silver grain. In Fig. 16a it can be said that the source corresponding to the silver grain marked "A" lies in the adjacent ferrite–ferrite interface because it lies well within the predicted value of the limit of resolution (1100 Å).

3.3. Reproducibility of results and background

We have experimentally verified the reproducibility of the technique by observing a large number of thin foil autoradiographs of each specimen. It is only by making such statistical observations that valid conclusions can be drawn. Observations have been made to ascertain the extent of the background; it was found to be negligible.

Figure 7 Microautoradiograph on the thin foil of a completely martensitic microstructure. (Specimen austenitized at 1025° C for 2 h and water-quenched). Silver filaments (marked by arrows) are randomly distributed with respect to the microstructure.

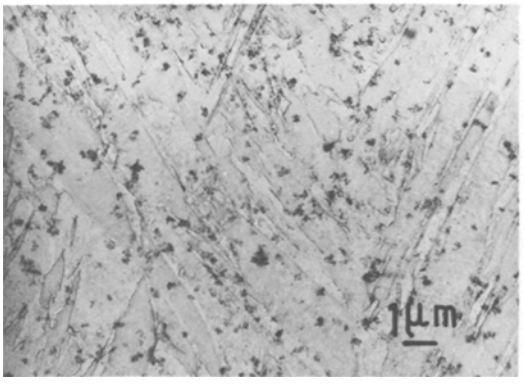

Figure 8 Autoradiograph on a massive specimen austenitized at 950° C for 2 h and water-quenched, showing apparently random distribution of silver grains on the fully martensitic microstructure.

4. Applications of the technique and some of the results obtained

The present work on a 12% chromium steel was undertaken with a view to studying the role of carbon in the evolution of the martensitic structure during tempering. Considerable work on the tempering behaviour of such steels has already been carried out by several authors using other experimental techniques [10–12].

The thin foil microstructure of a specimen austenitized at 1025° C for 2 h and quenched in water is shown in Fig. 1. A completely martensitic structure with a high density of dislocations is thus obtained. A high-resolution autoradiograph on a thin foil of this type of martensite is shown in Fig. 7. The random distribution of the silver grains reveals that the carbon is homogeneously distributed in such a structure. No segregation of carbon is observed at the original austenite grain boundaries. A similar distribution of carbon was also observed on the autoradiographs of the massive specimens (replicas) (Fig. 8). The replicas do not show enough microstructural details to derive precise conclusions. It may be observed that the use of thin foils instead of replicas offers a definite advantage in that the former permits a more precise localization of the radioactive tracer atoms with respect to the actual microstructural features.

It may be noted that a specimen austenitized at higher temperatures and quenched in water appears to show a segregation of carbon along the martensite interfaces (Fig. 9). The cause of this segregation of carbon has not yet been identified with certainty, but it may be due to the δ ferrite

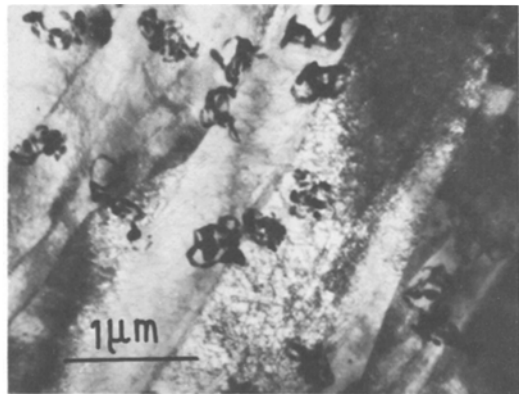

Figure 9 Microautoradiograph on the thin-foil microstructure of a specimen quenched in water from 1150° C, showing segregation of the silver filaments and hence that of carbon in the interfaces of the martensite laths.

since the specimen was austenitized in the $\delta + \gamma$ phase region.

On tempering, after austenitization at 1025° C for 2 h, and water-quench, the carbon held in super saturation is precipitated out. The morphology of the precipitates depends on the tempering temperature and time. Thus at temperatures up to about 500° C, needle-shaped precipitates appear in the martensitic laths (Fig. 10). These precipitates are carbides (probably M_7C_3), are thus rich in C*, and are marked by silver filaments.

At higher tempering temperature, about 550° C, globular precipitates, probably of the $M_{23}C_6$ type, appear mostly along the interfaces of the martensite laths and are also marked by silver filaments (Fig. 11).

Specimens tempered at 500° C for 18 h show the presence of both types of precipitates (Fig. 12). The M_7C_3 precipitates (needle-shaped precipitates labelled "a" in Fig. 12) contain a higher proportion of carbon than the $M_{23}C_6$ precipitates, but the former, being much smaller in dimensions, contain fewer radioactive carbon atoms and hence only the relatively large $M_{23}C_6$ type precipitates are marked by the silver grains in the autoradiograph.

In the specimens tempered at higher tempera-

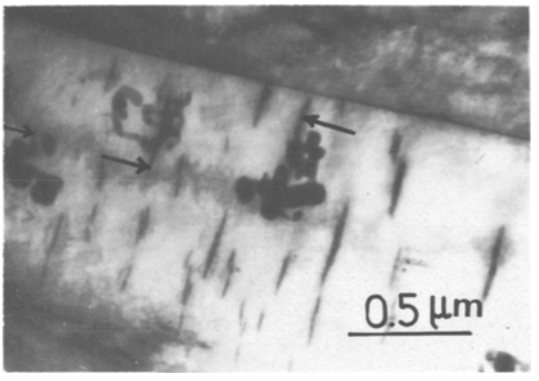

Figure 10 Autoradiograph on the thin-foil microstructure of a specimen tempered at 500° C for 1 h showing needle-shaped precipitates within the martensitic laths; some of the precipitates are marked by silver filaments (e.g. precipitates shown by arrows).

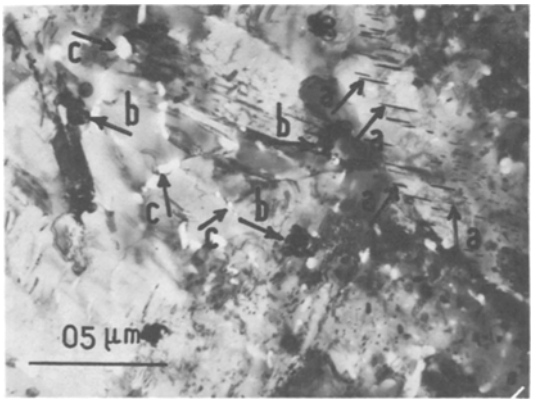

Figure 12 An autoradiograph on the thin-foil microstructure of a specimen tempered at 500° C for 18 h showing two types of precipitates. Rod-shaped precipitates are shown by arrows "a", and globular precipitates at the interfaces of the initial martensite, some of which are marked by silver filaments, are shown by arrows "b"; some of these precipitates have fallen into the bath during polishing (arrows "c").

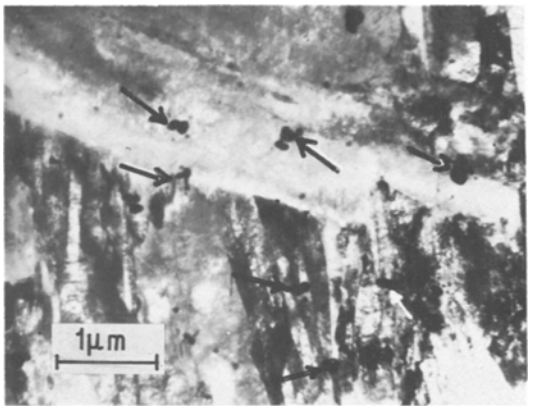

Figure 11 Autoradiograph on the thin-foil microstructure of a specimen tempered at 550° C for 1 h showing globular precipitates along the interfaces of the martensite laths, some of which are marked by silver filaments (the filaments superimposed on the precipitates are shown by arrows).

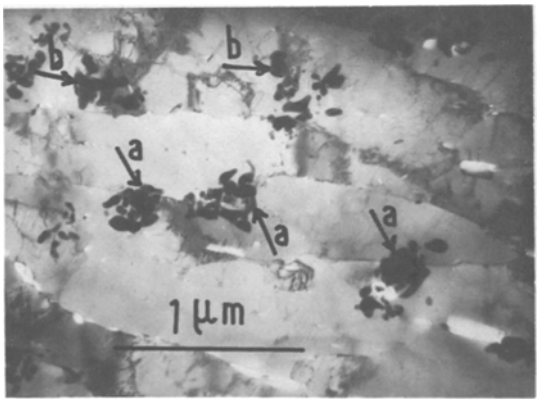

Figure 13 Autoradiograph on the thin-foil microstructure of a specimen tempered at 650° C for 20 h: (a) precipitates along the interfaces of the initial martensite, (b) precipitates along the ferrite–ferrite interfaces. Both types of precipitate are marked by silver filaments.

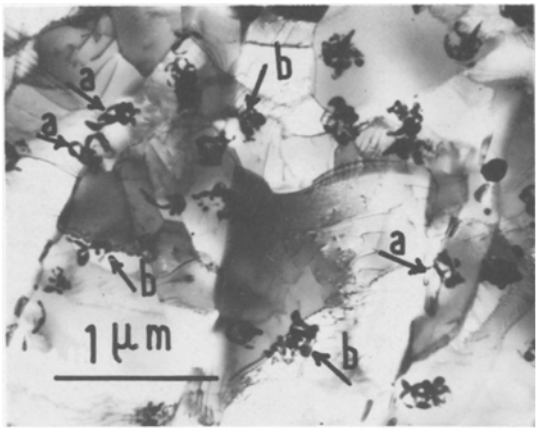

Figure 14 Autoradiograph on thin-foil microstructure of a specimen tempered at 700° C for 40 h: (a) precipitates along the interfaces of the initial martensite. (b) precipitates along the ferrite–ferrite interfaces.

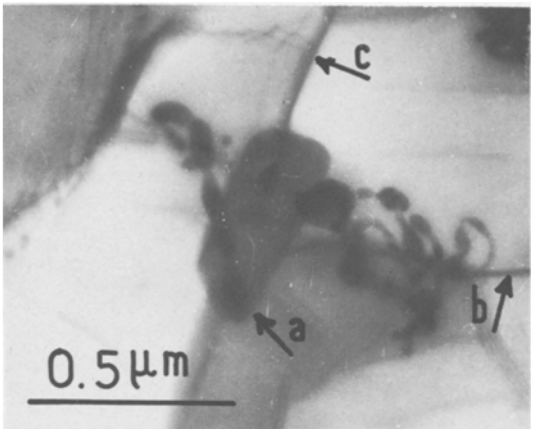

Figure 15 Autoradiograph on the thin-foil microstructure of a specimen tempered at 700° C for 40 h showing a large precipitate (shown by an arrow "a") at the intersection of ferrite–ferrite/martensite interfaces (shown by arrows "b" and "c" respectively).

tures (650° C, 20 h and 700° C, 40 h), the martensitic structure seems to have decomposed into a ferritic matrix and possibly only $M_{23}C_6$ type precipitates, occurring mostly along the interfaces of the initial martensite (shown by arrows "a" in Figs. 13 and 14). Similar precipitates also seem to occur along the ferrite–ferrite interfaces that have developed during tempering (shown by arrows "b" in Figs. 13 and 14). Relatively large precipitates appear to have precipitated along the intersections of the interfaces of the initial martensite and the ferrite–ferrite interfaces (Fig. 15). It may be noticed that there are certain ferrite–ferrite interfaces which show a concentration of carbon but do not show the presence of any precipitates (Fig. 16).

Specimens tempered at 750° C for 100 h also reveal a similar concentration of carbon in the elementary form along the subgrain boundaries (Fig. 16b). This indicates a possibility that the ferrite–ferrite interfaces happen to be the sites of carbon segregation and have possibly played an important role in assisting the elimination of carbon from the matrix during the evolution of the tempered structures. The concentration of carbon in these interfaces might have assisted the growth of the precipitates occurring on the intersections of these interfaces with the interfaces of the initial martensite, and might also have led to the precipitation of the carbides within the ferrite–ferrite interfaces themselves.

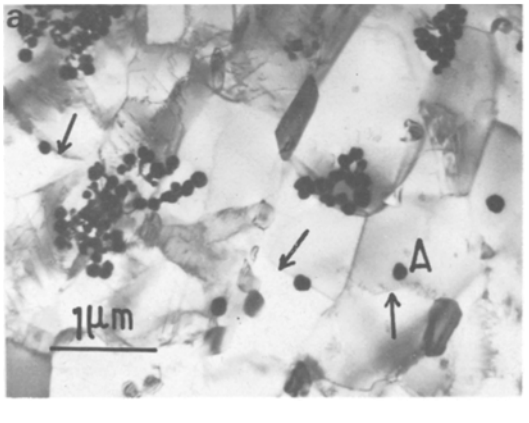

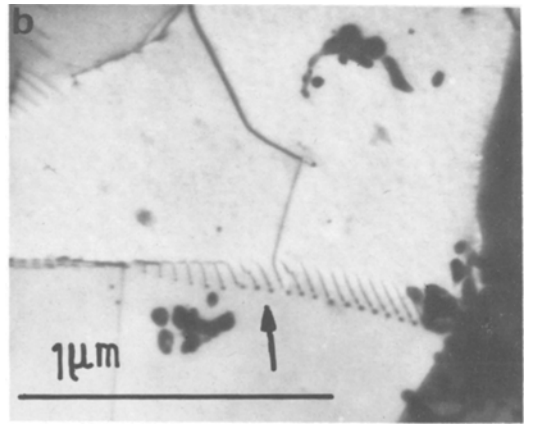

Figure 16 Autoradiographs on the thin-foil microstructure of specimens: (a) tempered at 700° C for 40 h, (b) tempered at 750° C for 100 h. The subgrain boundaries (shown by arrows) marked by silver grains reveal a segregation of carbon in atomic form without the presence of carbides in some of these interfaces.

The results obtained show that the technique of high resolution autoradiography on thin foils can be applied even to very complex structures, provided its limitations and merits are well understood. This technique can become an important tool to the physical metallurgist if suitably combined with other techniques; it offers a remarkable sensitivity to reveal heterogeneities in the distribution of the radioactive tracer atoms in a microstructure and permits the localization of the radioactive tracer atoms with respect to the microstructural features. It should be possible to apply this technique to study the role and the localization of carbon during other phase transformations and in different types of structures.

This technique can, in principle, be extended to investigate the role of other elements such as hydrogen [13, 14], sulphur, phosphorus etc, in various metallurgical phenomena, using appropriate isotopes.

5. Conclusions

(1) It is possible to obtain high-resolution electron microautoradiographs on thin foils, using a liquid nuclear emulsion. Such autoradiographs have many advantages over the autoradiographs on massive specimens (replicas). One of the advantages is that, in the former case more structural details can be observed since a specimen is observed by direct transmission electron microscopy.

Moreover autoradiographs using ^{14}C as a radioactive tracer give a much better resolution in the case of thin foils (3700 Å for a point source and 1300 Å for a continuous source) than in the case of massive specimens (replicas) (12 μm for a point source and 3.6 μm for a continuous source).

Determination of precise values of the efficiency r corresponding to a nuclear emulsion used and a photographic process adopted, may enable us to estimate the concentration of the radioactive tracer atoms in different sites of segregation (dislocations, subgrain boundaries, etc).

The technique is very sensitive and can reveal variations in the concentration of radioactive atoms with respect to the microstructural features to a remarkable extent.

(2) As-quenched martensitic structures show a homogeneous distribution of silver grains in the autoradiographs on massive specimens (replicas) as well as thin foils. Some segregation of carbon is observed along the interfaces of the martensite of a specimen austenitized at 1150° C, which probably contains an appreciable amount of δ ferrite. No segregation of carbon is found to exist in the original austenite grain boundaries.

After tempering, specimens show the presence of two types of precipitates: the first, needle-shaped precipitates, appear up to about 500° C within the martensite laths and are probably M_7C_3 type; the second, globular precipitates, appear at higher temperatures, above about 500° C, and are probably $M_{23}C_6$ precipitates; at first they are localized along the interfaces of the martensite laths. If the specimens are tempered at 650° C for 20 h and 700° C for 40 h, the $M_{23}C_6$ type precipitates appear along the initial martensite interfaces and also along the ferrite–ferrite interfaces developed during tempering.

Relatively large precipitates seem to occur at the intersections of ferrite–ferrite/initial martensite interfaces, showing a possibility that the former interfaces might have assisted in the growth of these precipitates. This mechanism is supported by the fact that some ferrite–ferrite interfaces, in a specimen tempered at 700° C for 40 h, show a segregation of carbon in the elementary form.

It will be possible to apply the technique of high-resolution electron micro-autoradiography applied to thin foils, using ^{14}C as a radioactive tracer, to investigate the role of carbon in the evolution of the martensitic structure during tempering. The technique will be of particular interest in investigating the role of carbon in the mechanism of phase transformations where the diffusion of the former plays an important role (e.g. bainitic transformations).

References

1. J. P. LAURENT and G. LAPASSET, *Int. J.A.R.I.* **124** (1973) 213; Report of D.G.R.S.T. contract 6801322 (1972).
2. A. M. HUNTZ, D. MARCHIVE, M. AUCOUTURIER and P. LACOMBE, *Int. J.A.R.I.* **24** (1973) 689.
3. A. M. HUNTZ and P. LACOMBE, *Canad. Met. Q.* **13** (1974) 155.
4. E. B. MIKUS and C. A. SIEBERT, *Trans. ASM* **50** (1958) 682.
5. G. C. TOWE, J. GROMBERG and J. W. FREEMAN, "High Resolution Autoradiography", NACA, Tech. note 3209 (1954).
6. M. A. KRISTAL, "Diffusion processes in iron alloys", Israel Program for scientific translations (Jerusalem, 1970) p. 121.
7. G. V. PRABHU GAUNKAR, A. M. HUNTZ and P. LACOMBE, *Metallography* **8** (1975) 257.
8. G. V. PRABHU GAUNKAR, A. M. HUNTZ, C.

SEVERAC and P. LACOMBE, *Mém. Sci. Rev. Met.* **71** (1974) 787.
9. A. W. ROGERS, "Techniques of Autoradiography" (Elsevier, New York, 1967).
10. R. L. RICKETT, W. F. WHITE, G. S. WALTON and J. C. BUTLER, *Trans. ASM* **44** (1952) 133.
11. K. J. IRVINE, D. J. CROWE and F. B. PICKERING, *J.I.S.I.* **195** (1960) 386.
12. B. R. BANERJEE, *ibid* **203** (1965) 166.
13. G. LAPASSET, Thèse Docteur Ingénieur, Université PARIS Sud (1975).
14. M. AUCOUTURIER, R. ASAOKA and G. LAPASSET, *Metallography*, to be published.

Received 14 January and accepted 8 February 1976.